Computational Aspects of Modeling Tokamak Disruptions with the NIMROD Code

Carl Sovinec,[1] Kyle Bunkers,[1] Brian Cornille,[1] Jacob King,[2] and Eric Held[3]

[1]*University of Wisconsin-Madison*

[2]*Tech-X Corporation*

[3]*Utah State University*

SciDAC-4 PI Meeting, July 23-24, 2018, Rockville, MD

Center for Tokamak Transient Simulation

Introduction: Disruption is an unplanned loss of plasma confinement; macroscopic dynamics are involved.

- Disruptions release stored energy over a short period of time.
  - Plasma thermal energy and energy in $\mathbf{B}_{pol}$ in ITER may be freed over ~1 ms and ~10s of ms, respectively.
  - ITER plasma will store > 500 MJ. (~100 kg of dynamite)
- Three concerns arise with disruption:

  1) Thermal loading, 2) EM loading, and 3) Runaway e^{-} generation

- Extreme conservatism is not an option.

  "Burning plasma operation in ITER will require … … small margins against each of the three major plasma operation limits …." Hender, *et al.*, NF **47**, S128 (2007).

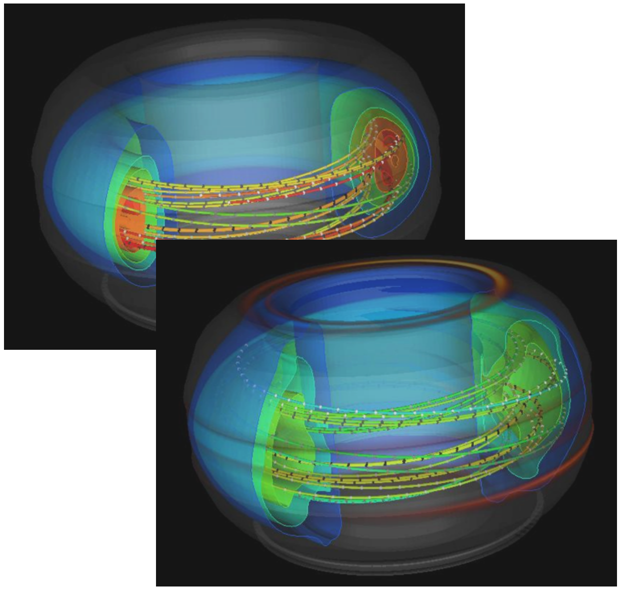

NIMROD high-β simulation results [Kruger, *et al.*, PoP **12**, 056113 (2005)].

Disruption is a multi-scale process.

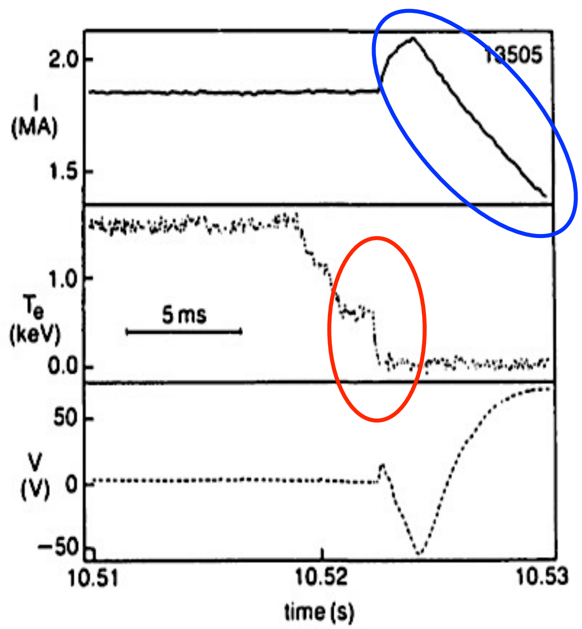

Density-limit disruption in limited JET. [Wesson, *et al*, NF **29**, 641 (1989)]

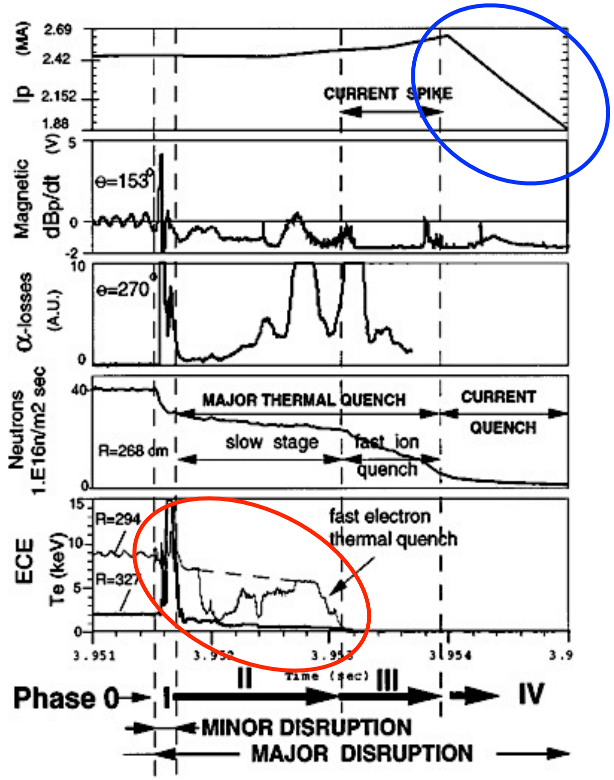

High-β disruption in TFTR. [Mirnov, *et al*, PoP **5**, 3950 (1998)]

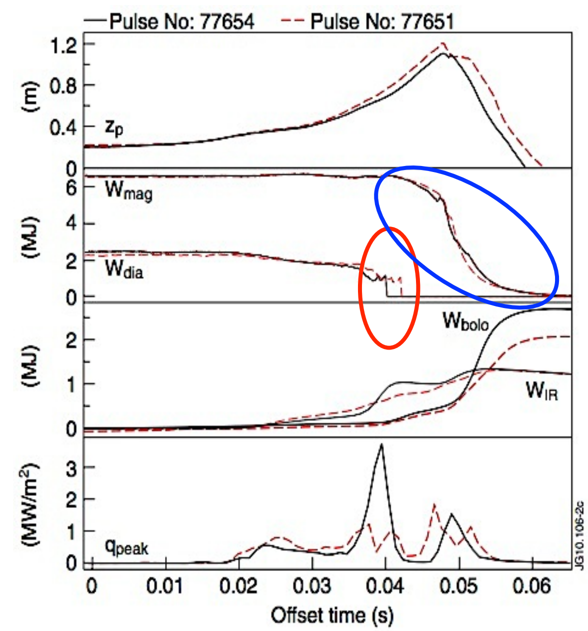

Forced VDE in diverted JET. [Riccardo, *et al*, PPCF **52**, 124018 (2010)]

- Thermal quench is circled in red; current quench (in blue) extends off first two plots.
- Note the distinct time-scales.

Simulations need to model the disruptive dynamics through the time that the discharge ends.

- Disruptions may excite multiple MHD events while the current decays.

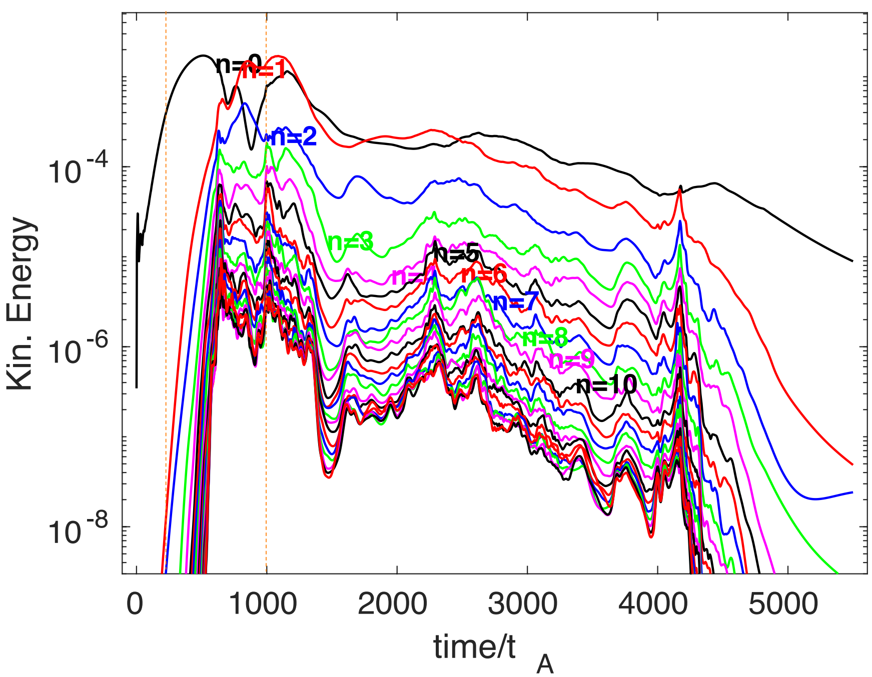

Simulated kinetic energy fluctuations decomposed by toroidal harmonic (0≤*n*≤21) indicate multiple events over time.

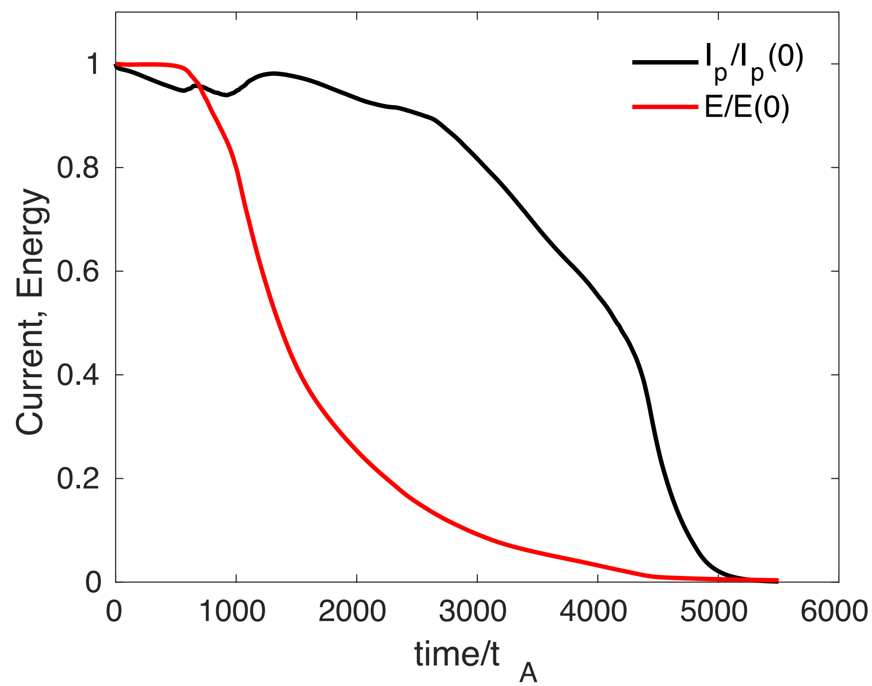

The simulation reproduces the qualitative effect of the TQ being fast relative to the CQ.

Disruption also involves multiple physical effects.

1. Macroscopic dynamics with **B**-topology evolution
   - Island evolution and stochasticity
   - Kink and vertical displacement
2. Kinetic-closure information
   - Perturbed bootstrap current for NTMs
   - Neoclassical viscosity for rotation damping
   - Parallel heat transport (TQ)
   - Cross-field transport
   - Fast-ion effects for RWMs
3. Runaway-electron kinetics
   - Distribution and confinement
   - Macroscopic effects on η during CQ
4. Impurity flows and radiation
   - Density-limit physics & TQ
   - Mitigation (gas and pellets)
   - Neutrals and charged species
5. Plasma-surface interaction
   - Sheath effects on currents, energy, and flows
   - Impurity sourcing

- Present efforts represent a start on integrated disruption simulation.

Disruption can include one or more classes of macroscopic plasma dynamics.

Magnetic Topology Change:

- Resistive or other non-ideal instabilities reconnect magnetic field-lines and develop topologically distinct magnetic islands.
- Island overlap produces regions of stochastic magnetic field.
- Islands also tend to brake plasma flows, leading to secondary instabilities.

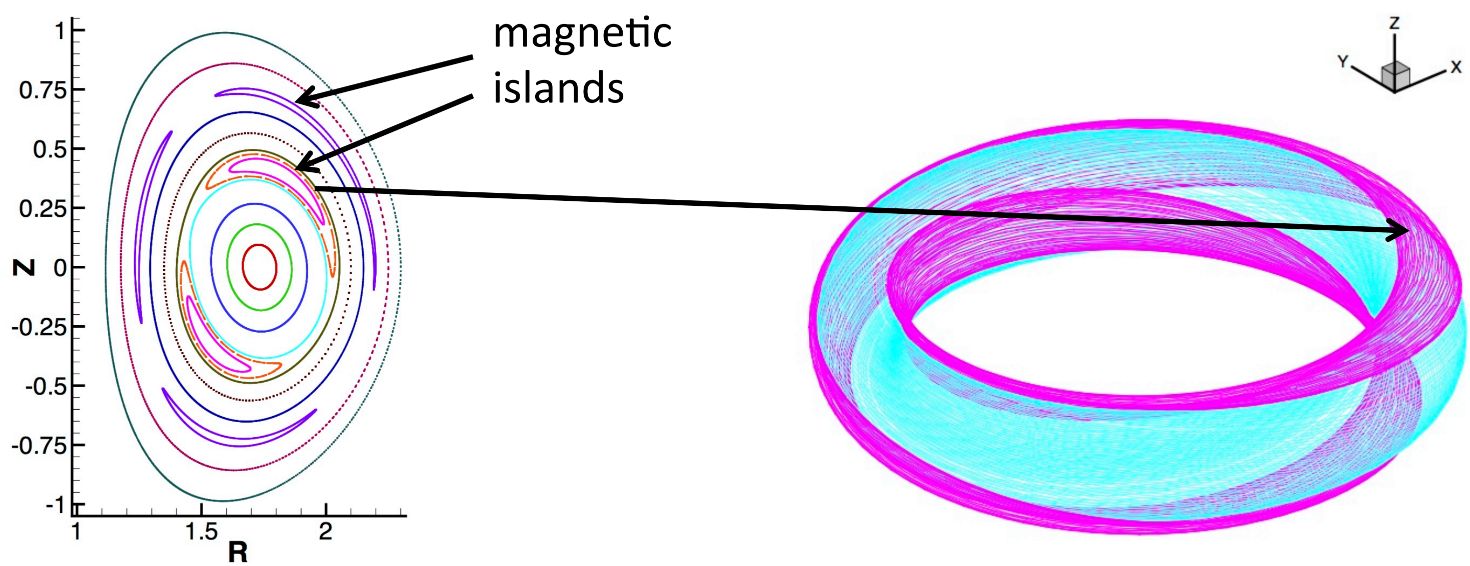

Cross-sections of islands are embedded among toroidal flux surfaces.

Non-overlapping islands are distinct regions but enhance energy transport.

Vertical displacement of the plasma torus leads to wall contact.

Vertical Displacement:

- Modern tokamak plasmas are vertically elongated, which stabilizes some macroscopic modes but requires active vertical position control.
- Disruptive transients can upset this control.
- Control can also be lost without other instabilities.

Vertical-displacement simulation results show evolution of plasma pressure (color) and magnetic flux.

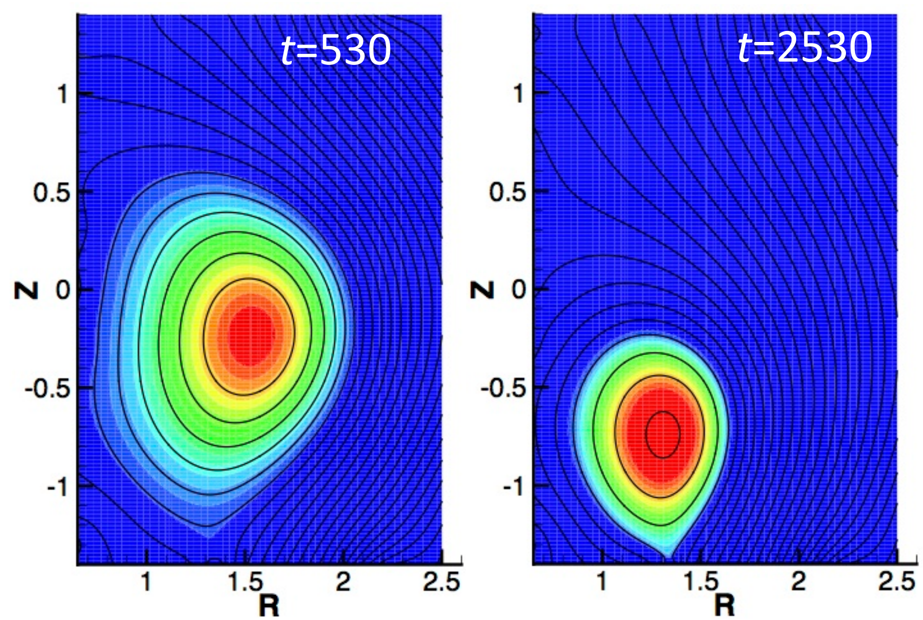

Three-dimensional distortion of the plasma shape results from kink instability.

Kink distortions:

- Kink instability can result from insufficient profile control.
- Loss of plasma flow due to island-induced braking destabilizes kink that grows on the time-scale of resistive diffusion through the wall.
- Contact with a surface during vertical displacement also destabilizes kink.

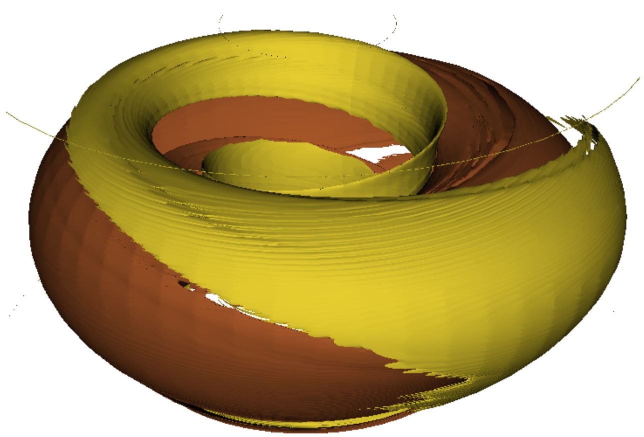

Isosurfaces of $J_{||}/B$ = -0.085 (mustard) and $J_{||}/B$ = +0.8 (brown) from a toroidal simulation showing kink instability.

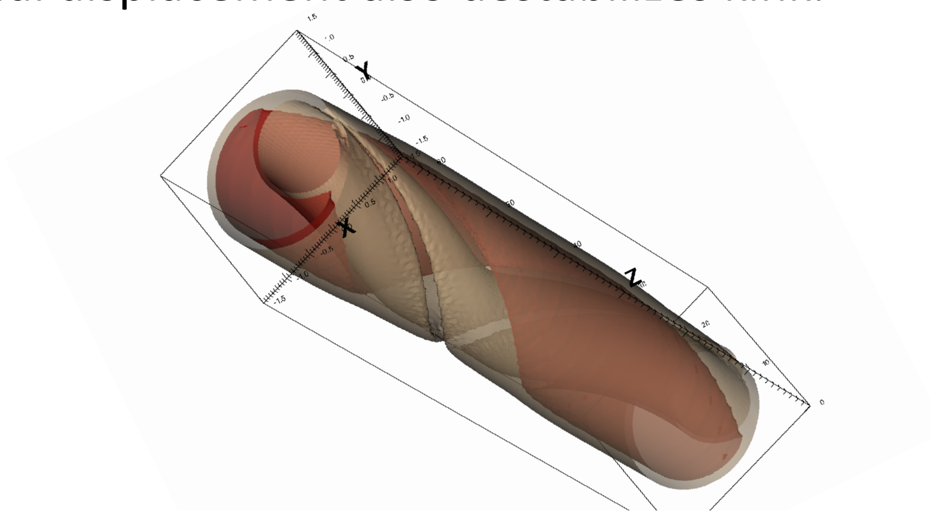

Particle density isosurfaces at 25% (tan) and 75% (red) of max from computational results of idealized bubble-swallowing.

Model: Our computations use visco-resistive (full) MHD with fluid closures.

- The following system is our base non-ideal single-fluid model.

$\frac{\partial n}{\partial t} + \nabla \cdot (n\mathbf{V}) = \nabla \cdot \left(D_n \nabla n - D_h \nabla \nabla^2 n \right)$	particle continuity with artificial diffusion
$mn\left(\frac{\partial}{\partial t} + \mathbf{V} \cdot \nabla \right)\mathbf{V} = \mathbf{J} \times \mathbf{B} - \nabla(2nT) - \nabla \cdot \underline{\Pi}$	momentum density
$\frac{n}{\gamma - 1}\left(\frac{\partial}{\partial t} T + \mathbf{V} \cdot \nabla T \right) = -nT\nabla \cdot \mathbf{V} - \nabla \cdot \mathbf{q}$	temperature evolution
$\frac{\partial \mathbf{B}}{\partial t} = -\nabla \times (\eta \mathbf{J} - \mathbf{V} \times \mathbf{B})$	Faraday's law & MHD Ohm's
$\mu_0 \mathbf{J} = \nabla \times \mathbf{B}$	Ampere's law
$\nabla \cdot \mathbf{B} = 0$	divergence constraint

- The NIMROD code (https://nimrodteam.org) is used to solve linear and nonlinear versions of this system.

Closure relations approximate plasma transport effects.

- Magnetic diffusivity depends on temperature.
  - $\eta(T) = \eta_0 (T_0/T)^{3/2}$
- Thermal conduction and viscous stress are anisotropic to approximate magnetization of plasma particles.
  - $\mathbf{q} = -n\left[(\chi_{\|} - \chi_{iso})\hat{\mathbf{b}}\hat{\mathbf{b}} + \chi_{iso}\underline{\mathbf{I}}\right] \cdot \nabla T$
  - $\underline{\Pi} = \nu_{\|} mn\left(\underline{\mathbf{I}} - 3\hat{\mathbf{b}}\hat{\mathbf{b}}\right)\hat{\mathbf{b}} \cdot \underline{\mathbf{W}} \cdot \hat{\mathbf{b}} - \nu_{iso} mn\underline{\mathbf{W}}$ $\qquad \underline{\mathbf{W}} = \nabla\mathbf{V} + \nabla\mathbf{V}^T - \frac{2}{3}\underline{\mathbf{I}}\nabla \cdot \mathbf{V}$
  - $\chi_{\|}/\chi_{iso} >> 1 \qquad \nu_{\|}/\nu_{iso} >> 1$
- Temporal scales are well separated.
  - $\tau_{\text{Alfven waves}} << \tau_{\text{wall diffusion}} << \tau_{\text{plasma resistive diffusion}}$
  - Different disruptive dynamics occur over ranges of timescales: 100s of τ_A to many τ_w.

Kinetic information can be incorporated through closures on the fluid-moment equations.

- Evolution of “single-particle” distribution function (~ probability density function) is averaged over gyro-angle.
  - $\frac{\partial \bar{f}}{\partial t} + \dot{\mathbf{x}}_{gc} \cdot \nabla \bar{f} + \dot{s}\frac{\partial \bar{f}}{\partial s} + \dot{\xi}\frac{\partial \bar{f}}{\partial \xi} = C$ [Held, *et al.*, PoP **22**, 032511 (2015)]
  - s is normalized speed, and ξ is cosine of pitch-angle wrt **B**.
  - The distribution function is in 5D space + time, $\bar{f} = \bar{f}\left(\mathbf{x}, s, \xi, t\right)$.
  - C is the collision operator, which is second-order in s-ξ space.
- Gyro-averaging eliminates a sixth dimension but complicates the PDE.
  - $\left(\dot{\mathbf{x}}_{gc}, \dot{s}, \dot{\xi}\right)$ is the velocity vector for characteristic trajectories in 5D, and it depends on **E**, **B**, *T*, s, and ξ.

Numerics: the NIMROD code uses 2D spectral elements over a plane and 1D finite Fourier series for the periodic coordinate.

- Spectral elements[1] are finite elements where the polynomial degree of the basis functions may be arbitrarily large.
- Functions may be expanded in orthogonal polynomials or in equivalent cardinal functions.
- In NIMROD, these elements allow accurate representation [JCP **195**, 355] of
  - extremely anisotropic transport and
  - the magnetic divergence constraint without mesh alignment.

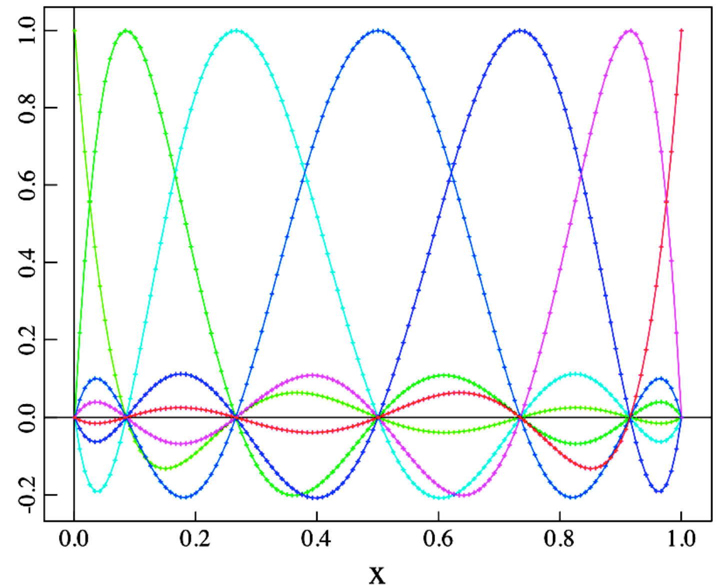

Example of cardinal basis functions for interpolation: Lobatto grid from the Legendre polynomial of degree 7.

[1]Boyd, *Chebyshev and Fourier Spectral Methods*; Deville, Fischer, and Mund, *High-order Methods for Incompressible Fluid Flow.*

The time-advance is tailored for magnetized plasma dynamics.

- NIMROD's implicit leapfrog [Sovinec and King, JCP **229**, 5803] advances different physical fields in separate algebraic systems.
- This method is an extension of earlier semi-implicit methods for waves.
  - It was developed for Hall-MHD computation.
  - Advection is implicit.

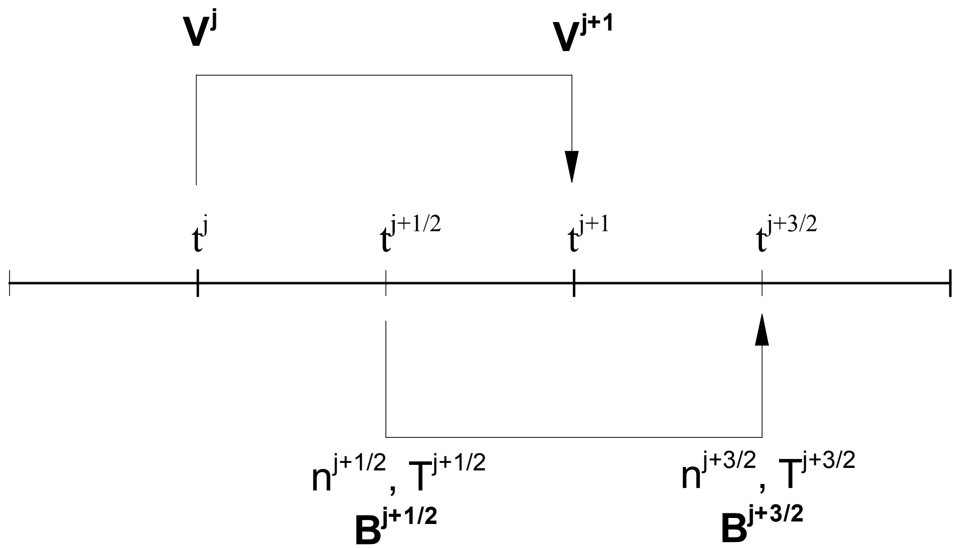

The plasma flow velocity is temporally staggered, hence "leapfrog."

- The C^0 representation is stabilized by the semi-implicit operator, by divergence-error diffusion, and by spectral projections of parallel vorticity and compression [Sovinec, JCP **319**, 61 (2016)].

We are investigating first-order system, least-squares to help stabilize the representation.

- Direct application of least-squares includes Navier-Stokes, MHD, and two-fluid systems.
  - Bochev and Gunzberger (Comput. Fl. **22**, 549) tested LS for NS.
  - Cai, *et al*. (SIAM JNA **31**, 1785) analyze first-order system LS formulations.
  - Adler, *et al*. (SIAM JSC **32**, 229) apply FOSLS to incompressible resistive MHD.
  - Leibs and Manteuffel (SIAM JSC **37**, S314) develop a two-fluid version.
- Least-squares has also been used for separate stabilizing terms.
  - Stabilization of the Galerkin formulation results from least-squares minimization of intra-element residuals.
  - Hughes and Franca (CMAME **65**, 85) introduced LS for Stokes flow (viscous and incompressible).
  - Barth, *et al.* (SIAM JSC **25**, 1585) compares different approaches.
  - Hughes, Franca, and Hulbert (CMAME **73**, 173) extend the approach to the advection-diffusion equation.

The implicit continuity equation has no physical dissipation and benefits from least-squares stabilization.

- Define the local residual for an arbitrary function f in the space for Δn as:

$$R = f + \Delta t \left\{ \left(\frac{f}{2} + n^{j+1/2} \right) \nabla \cdot \left(\mathbf{V}_s + \mathbf{V}^{j+1} \right) + \left(\mathbf{V}_s + \mathbf{V}^{j+1} \right) \cdot \nabla \left(\frac{f}{2} + n^{j+1/2} \right) + n_s \nabla \cdot \mathbf{V}^{j+1} + \mathbf{V}^{j+1} \cdot \nabla n_s \right\}$$

- LSQ minimizes the error.
  - Find $\Delta n \in N$ that minimizes *I*, where $I = \int R^2 \, dVol$
  - The algebraic equation results from varying Δn->*g* within the space. For all $g \in N$, find Δn such that

$$\delta I = 0 = 2 \int dVol \left[\Delta n + \Delta t \left\{ \left(\frac{\Delta n}{2} + n^{j+1/2} \right) \nabla \cdot \left(\mathbf{V}_s + \mathbf{V}^{j+1} \right) + \left(\mathbf{V}_s + \mathbf{V}^{j+1} \right) \cdot \nabla \left(\frac{\Delta n}{2} + n^{j+1/2} \right) + n_s \nabla \cdot \mathbf{V}^{j+1} + \mathbf{V}^{j+1} \cdot \nabla n_s \right\} \right] \times \left[g + \Delta t \left\{ \frac{g}{2} \nabla \cdot \left(\mathbf{V}_s + \mathbf{V}^{j+1} \right) + \left(\mathbf{V}_s + \mathbf{V}^{j+1} \right) \cdot \nabla \left(\frac{g}{2} \right) \right\} \right]$$

Simple advection tests without dissipation show that least-squares reduces noise.

- 1D tests consider 20 cubic elements with uniform flow in a periodic domain.

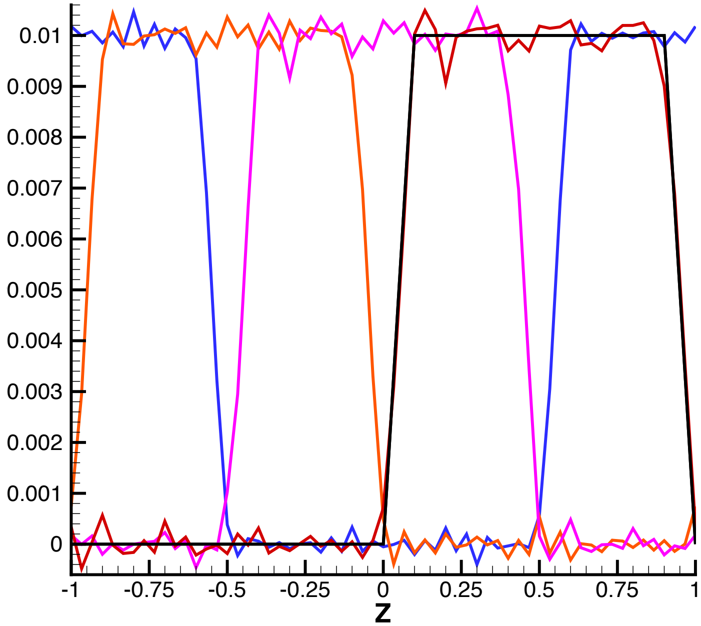

Advection without dissipation produces mesh-scale noise with Galerkin projection. (CFL=0.47)

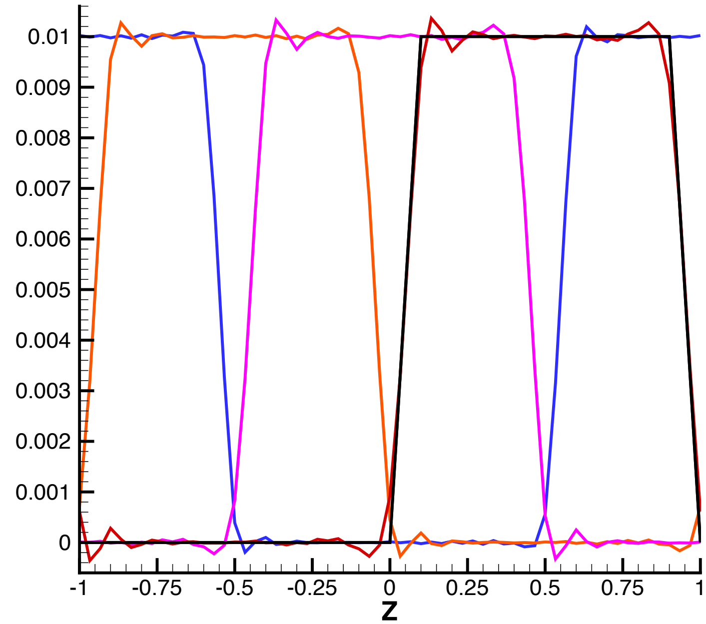

Least-squares projection avoids noise but does not prevent overshoot.

- Least-squares for *n* and *T* has been used in disruption simulations.

Least-squares may also benefit the advance of magnetic field in Hall-MHD computations.

- Here $\mathbf{E} = \eta\mathbf{J} - \mathbf{V}\times\mathbf{B} + (ne)^{-1}(\mathbf{J}\times\mathbf{B} - \nabla P_e)$ and the **J**x**B** Hall term is, effectively, advective.
- An auxiliary field is needed for first-order least-squares, and the cleanest system will need an *H*(curl) representation for **E** (or **A**):

Minimize $I = \int dVol\left[\mathbf{R}_B\cdot\mathbf{R}_B + CR_d^2 + C_E\mathbf{R}_E\cdot\mathbf{R}_E\right]$ for

$$\mathbf{R}_B = \Delta\mathbf{b} + \Delta t\nabla\times\mathbf{e}$$

$$R_d = \nabla\cdot(\mathbf{b} + \Delta\mathbf{b})$$

$$\mathbf{R}_E = \mathbf{e} + \mathbf{K}\times(\mathbf{b} + f\Delta\mathbf{b}) + f\,\mathbf{L}\times\nabla\times\Delta\mathbf{b} - f\frac{(\eta_0 + \tilde{\eta})}{\mu_0}\nabla\times\Delta\mathbf{b} - \mathbf{M}$$

with $\{\Delta\mathbf{b},\mathbf{e}\}\in S_{\mathbf{B}3} = H^1\times H(\mathrm{curl})$, and **K**, **L**, and **M** are known vectors during the computation for **e** and Δ**b**.

Parallel computing: NIMROD fluid computations use 3D domain decomposition over spatial coordinates.

- Data structures for NIMROD's 2D mesh of elements are divided into blocks.
  - Block are mapped to processes for MPI parallelization.
  - Hybrid parallelization via OpenMP is also based on the block decomposition.
  - Blocks enhance geometric flexibility.
- Fourier components for the 3rd dimension are decomposed among layers of processors.
  - Communication is used before and after FFTs.

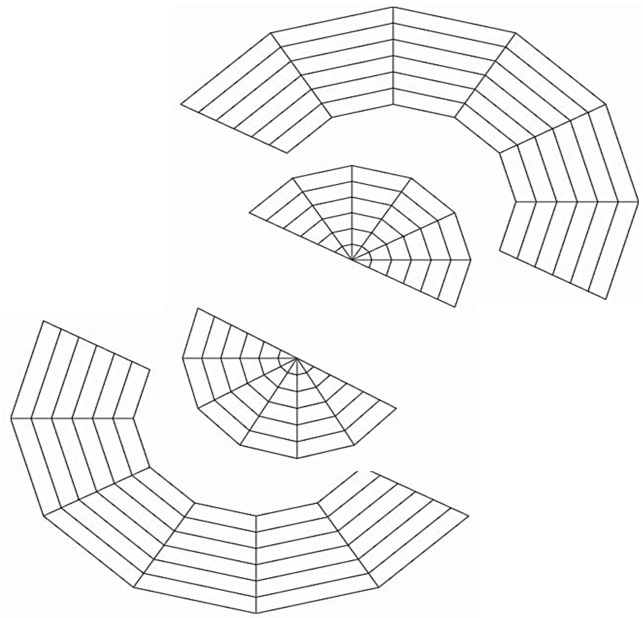

Heuristic representation of 2D decomposition of elements.

Tests of hybrid parallelization on NERSC's Cori KNL show competing computational needs.

- Tests use a large element mesh but do not emphasize factorization or Fourier-based parallelization.

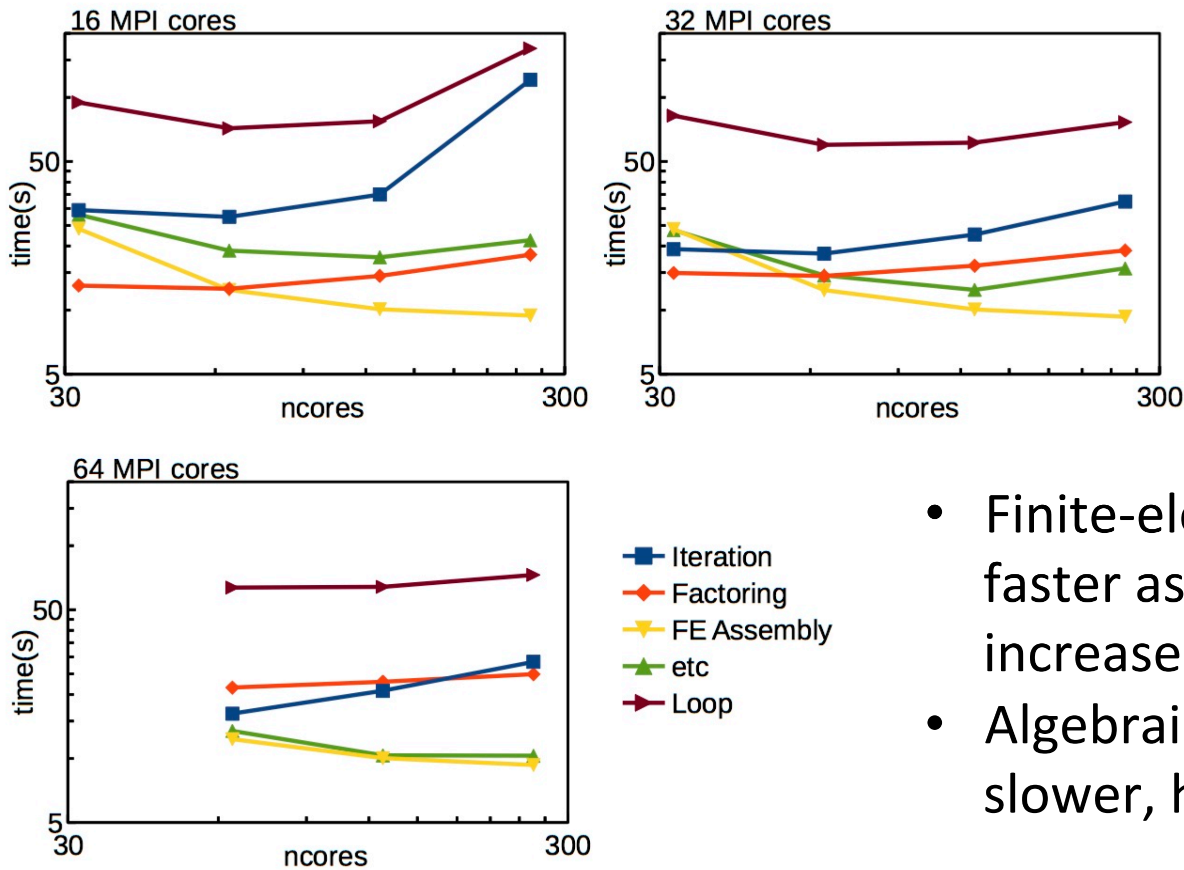

- Finite-element assembly is faster as threading is increased.
- Algebraic solves tend to get slower, however.

Recent work adds parallel decomposition over the speed grid in kinetic computations.

- Magnetic islands lead to enhanced thermal transport.
- In high-temperature, low-collisionality plasma, heat flux results from significant distortions of the particle distribution function.

- Coupling over particle-speed grid is relatively weak.
- MPI decomposition has been applied over this coordinate.

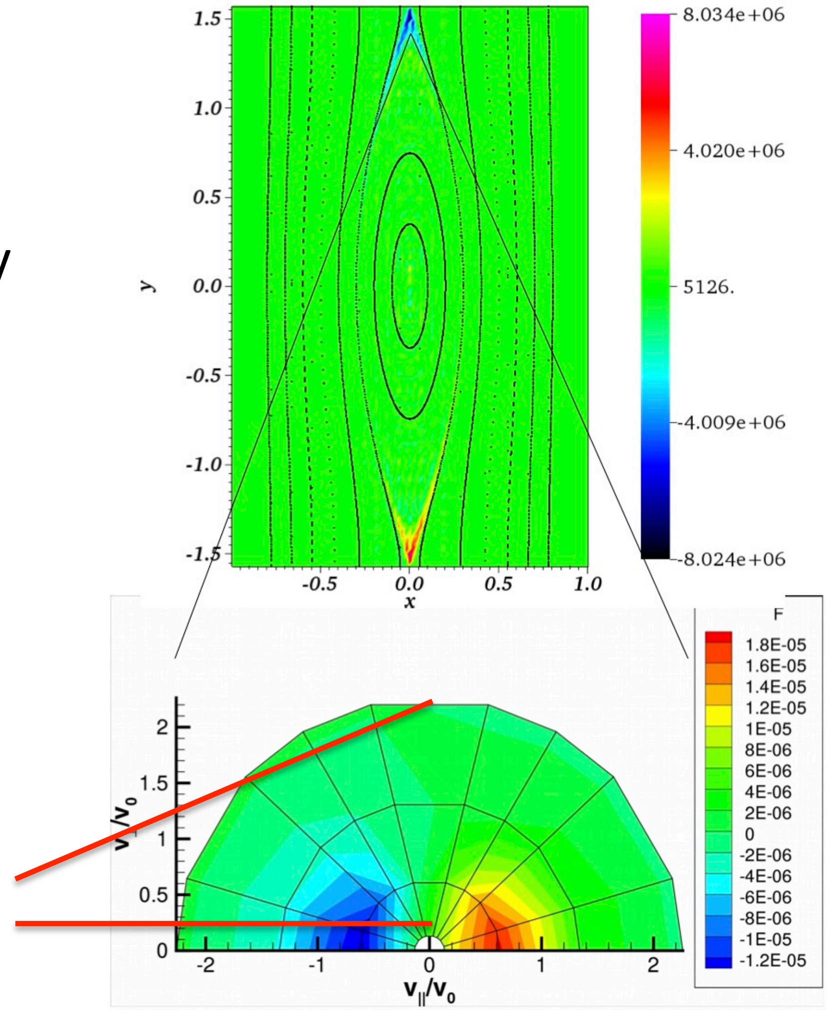

Computed results on distortion of distribution (lower frame), due to island (above).

Parallel decomposition over the speed grid facilitates kinetic modeling.

- Computations within individual speed values dominate processing time.
- Weak scaling with the new decomposition, assigning a single speed value to each group of processors, shows practical performance gains.

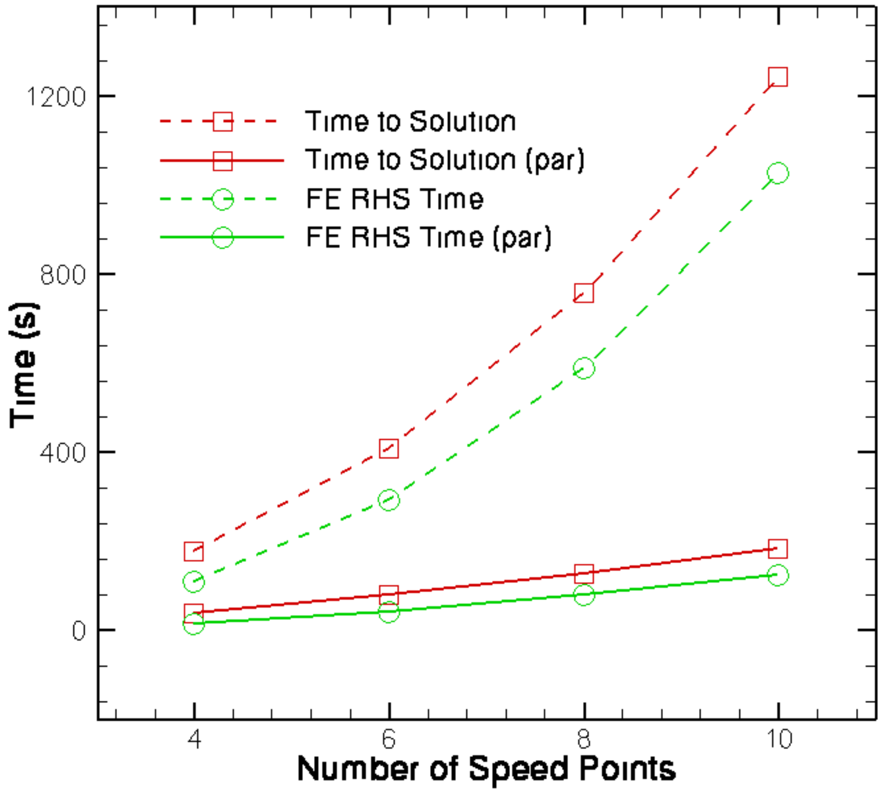

Speed-parallelization weak-scaling results are shown by the solid lines.

Algebraic solves: Parallel linear algebra tends to dominate overall computational performance.

- Global-scale physical propagation of information over each time-step leads to ill-conditioned algebraic systems.
- Algebraic systems for nonlinear computations couple all 2D element nodes and all Fourier components.
  - Meshes for large fluid-model computations are of order 1M nodes and 20-100 Fourier components.
  - Kinetic computation adds two smaller dimensions.
  - The size of Fourier-off-diagonal terms depends on the amplitude of the perturbations.
- Preconditioned GMRES and CG are used to solve the algebraic systems.
  - Fourier coupling is based on matrix-free computation.

Preconditioning is based on sparse direct solves over the 2D spatial mesh.

- Standard preconditioning is block-Jacobi with blocks extending over the 2D mesh of elements.
- SuperLU_DIST [Li and Demmel, ACM TMS **29**, 110] is used in nearly all parallel computations.

$$\begin{bmatrix} \Box & \Diamond & \copyright & \flat & \bigstar \\ \clubsuit & \Box & \spadesuit & \ddagger & \ominus \\ \otimes & \maltese & \Box & \oplus & \sqcup \\ * & \aleph & \uplus & \Box & \wedge \\ \blacklozenge & \triangledown & \trianglelefteq & \heartsuit & \Box \end{bmatrix} \rightarrow \begin{bmatrix} \Box & 0 & 0 & 0 & 0 \\ 0 & \Box & 0 & 0 & 0 \\ 0 & 0 & \Box & 0 & 0 \\ 0 & 0 & 0 & \Box & 0 \\ 0 & 0 & 0 & 0 & \Box \end{bmatrix}$$

Schematic of block-Jacobi. For NIMROD each block is all nodal degrees of freedom for a single Fourier harmonic.

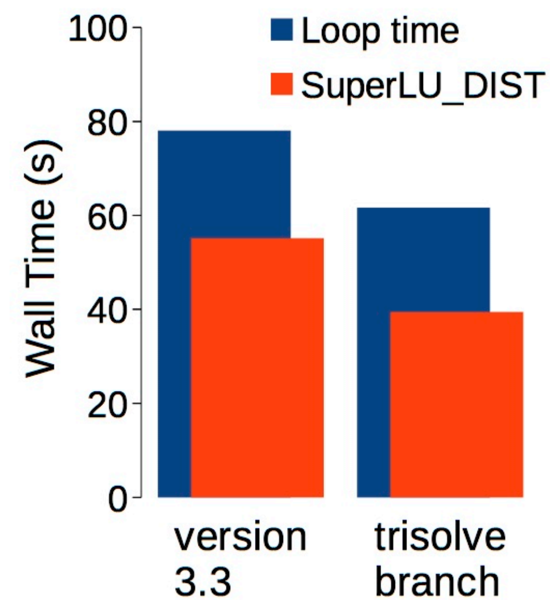

Xiaoye Li of LBL applied her reduced-latency method to NIMROD on KNL.

Preconditioning toroidally distorted conditions is a challenge for disruption computations.

- A limited block-Gauss Seidel operation improves robustness in only some computations.

$$\begin{bmatrix} \square & \diamond & 0 & 0 & 0 \\ \clubsuit & \square & \spadesuit & 0 & 0 \\ 0 & \maltese & \square & \oplus & 0 \\ 0 & 0 & \uplus & \square & \wedge \\ 0 & 0 & 0 & \heartsuit & \square \end{bmatrix} \xrightarrow{\text{for each block equation}} \left[(\mathbf{L} + \mathbf{D})\mathbf{x}_{\text{new}} = \mathbf{r} - \mathbf{U}\mathbf{x}_{\text{old}} \right]$$

- Alternating between two preconditioners (FGMRES), where the second is based on physical planes, also helps in some cases.

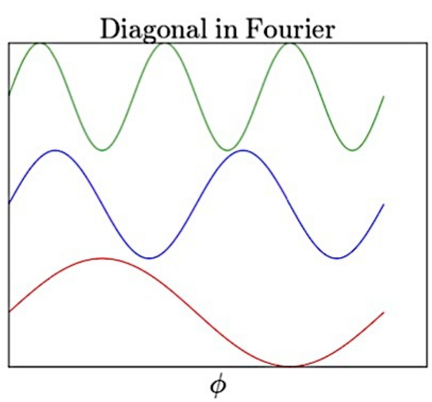

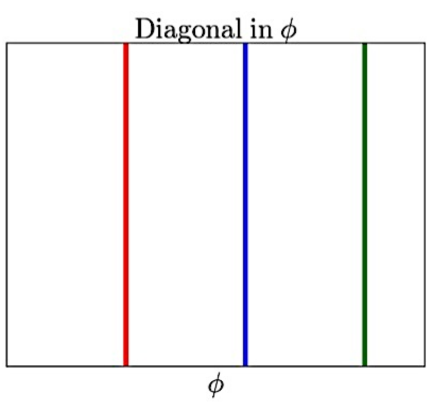

Conclusions and Outlook

- Understanding disruptions through numerical simulation is important for the magnetic confinement program.
- The multi-scale, multi-physics nature of tokamak disruption influences the choice of suitable numerical methods.
- Disruption simulation studies with the NIMROD code are progressing through continuous improvement of
  - Physics models,
  - Numerical methods,
  - Algebraic solvers, and
  - Use of new computer architectures.